Electronic Supplementary Material (ESI) for Analyst.

Supporting Information

Nitro-functionalized Metal–organic Frameworks with Catalase Mimic Properties for Glutathione Detection

Jiayan Wang,[ab] Wenying Li,[a]* Yue-Qing Zheng[a]*

[a]Chemistry Institute for Synthesis and Green Application, School of Materials Science and Chemical Engineering, Ningbo University, Ningbo 315211, Zhejiang, PR China.

[b]Medical School, Ningbo University, Ningbo 315211, Zhejiang, PR China.

*Corresponding author:

Email: liwenying@ nbu.edu.cn (W. Li), zhengyueqing@nbu.edu.cn (Y-Q. Zheng)

Fax: +86-574-87600789

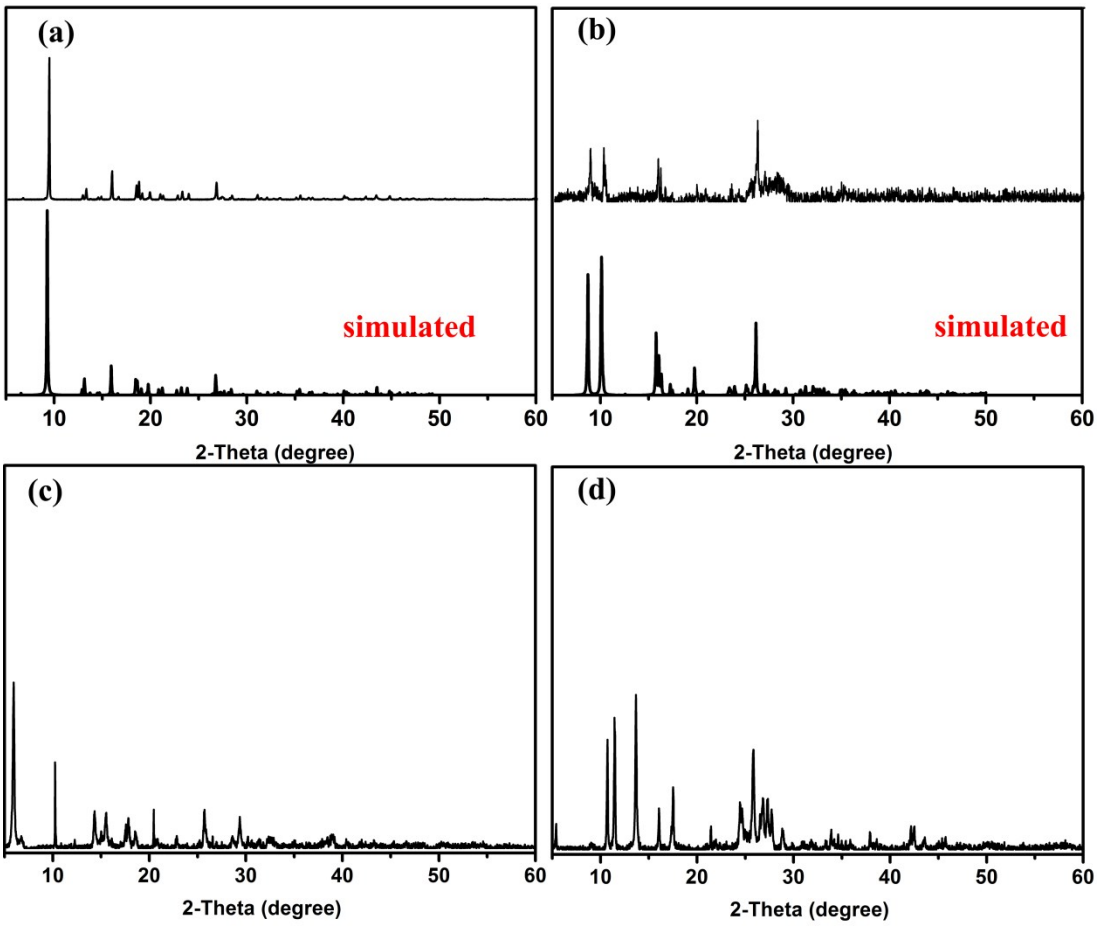

Figure S1. XRD patterns of (a) Cu-MOFs (i), (b) Cu-MOFs (ii), (c) Cu-MOFs (iii), (d) Cu-MOFs (iv).

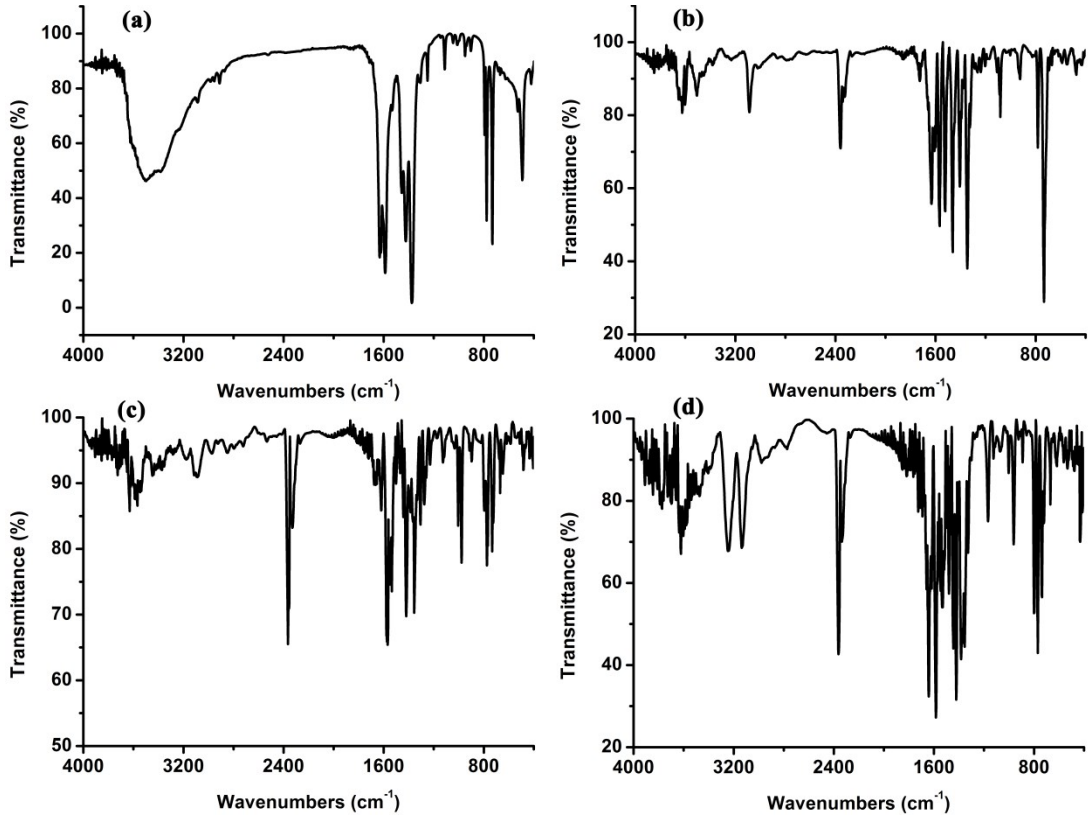

Figure S2. FTIR spectrum of (a) Cu-MOFs (i), (b) Cu-MOFs (ii), (c) Cu-MOFs (iii), (d) Cu-MOFs (iv).

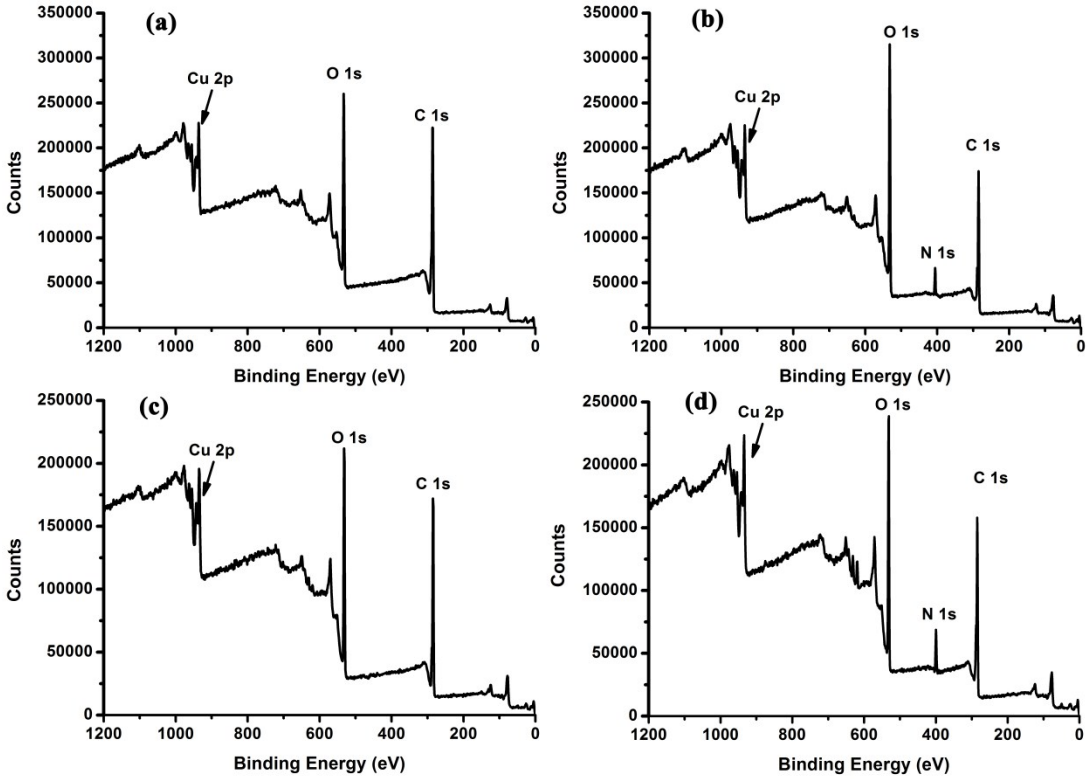

Figure S3. Survey XPS (a) Cu-MOFs (i), (b) Cu-MOFs (ii), (c) Cu-MOFs (iii), (d) Cu-MOFs (iv).

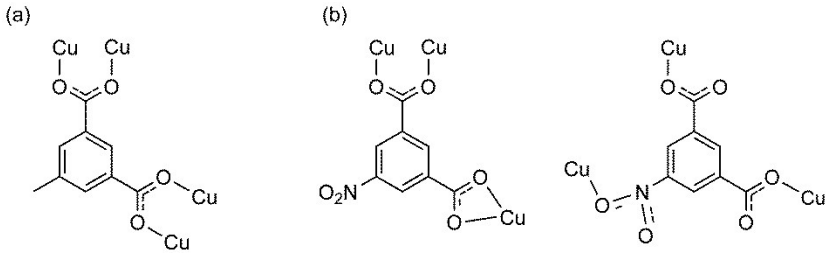

Figure S4 Coordination Modes of ligand i (a) and ligand ii (b) with Cu^{2+}.

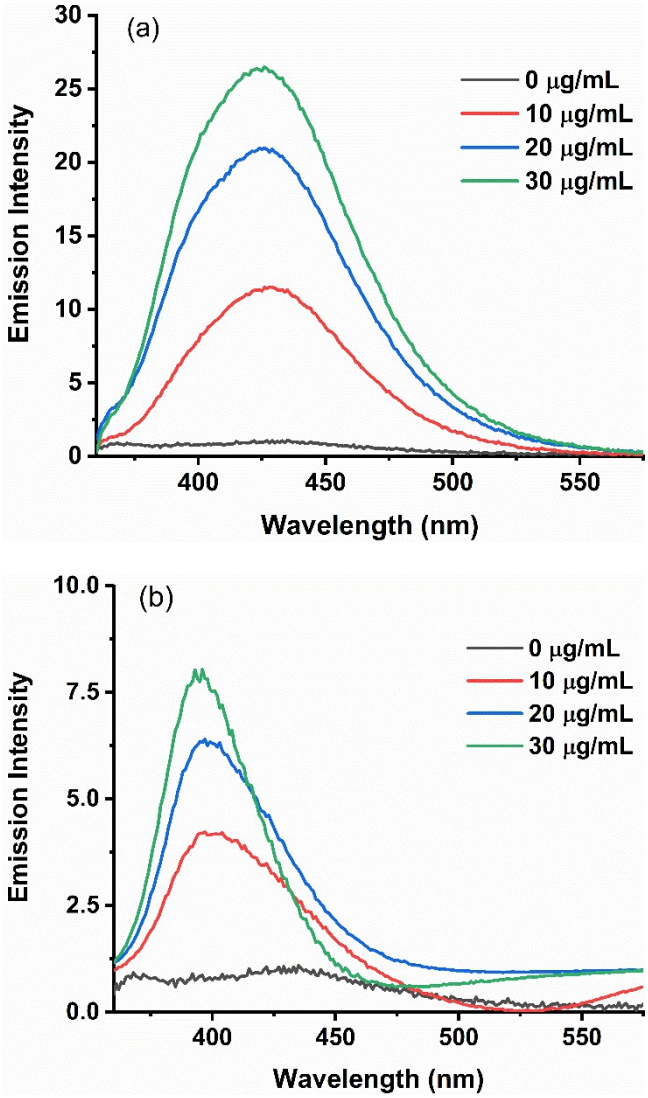

Figure S5. Effects of (a) Cu-MOFs (i) and (b) Cu-MOFs (iv) on the changes of hydroxyl radicals with terephthalic acid as the fluorescence probe. Assay conditions: 5 μM terephthalic acid, 4 mM H_2O_2, pH 7.0, 5 min. The emission intensity of Cu-MOFs (iv) itself was subtracted.

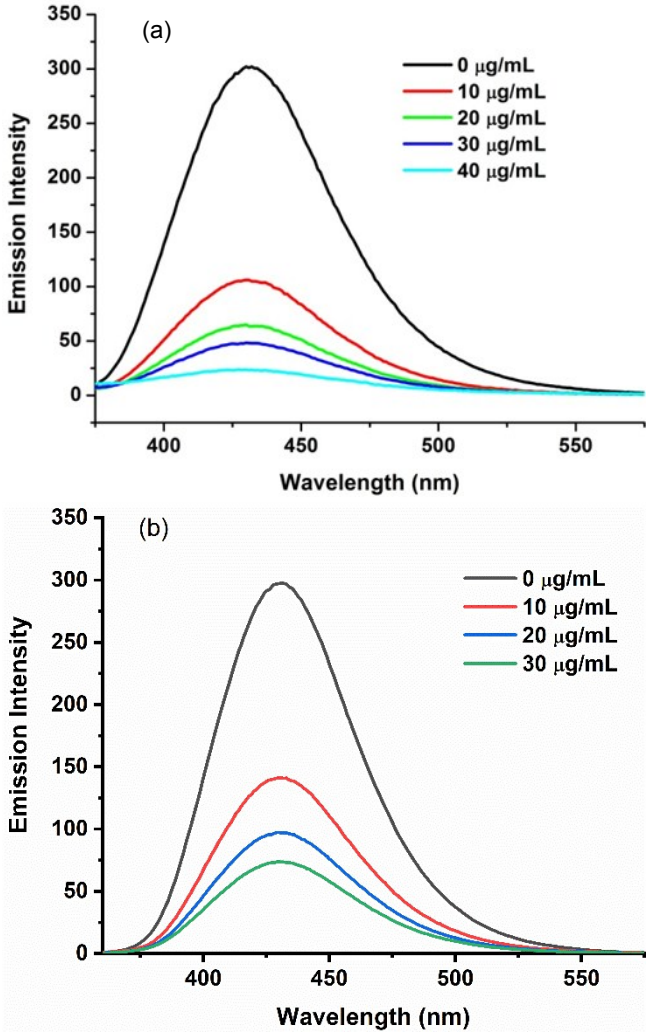

Figure S6. Effects of (a) Cu-MOFs (ii) or (b) Cu-MOFs (iii) on the changes of hydroxyl radicals with terephthalic acid as the fluorescence probe. Assay conditions: 5 μM terephthalic acid, 4 mM H_2O_2, pH 7.0, 5 min.

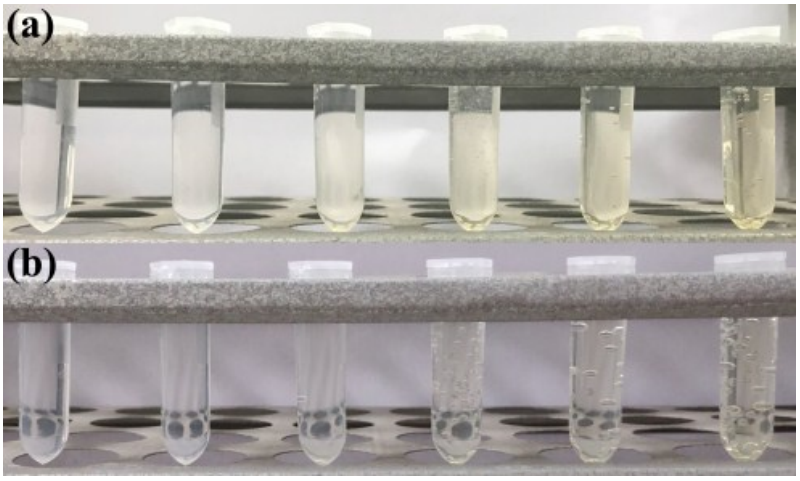

Figure S7. Photograph of gas bubble generated by the decomposition of H_2O_2 in pH 7.0. (a) Reaction for 30 minutes. (b) Reaction for 60 minutes. From left to right, the concentrations of Cu-MOFs (ii) were 0, 10, 20, 30, 40 and 50 μg/mL respectively.

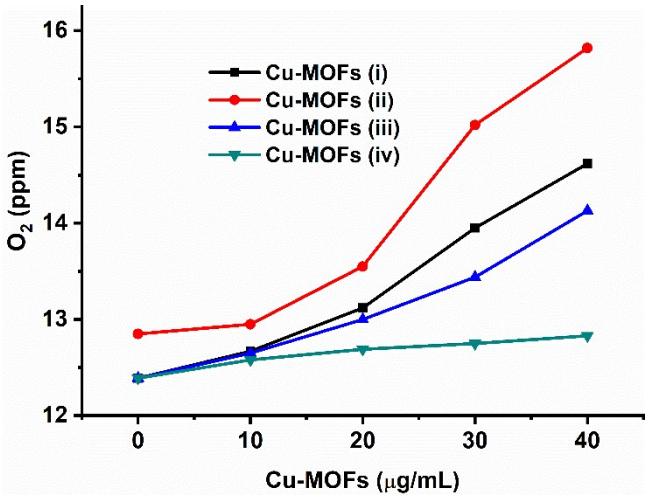

Figure S8. Effect of Cu-MOFs (ii) concentration on the generation of O_2 by the decomposition of H_2O_2. Assay conditions: 4 mM H_2O_2 and different concentrations of Cu-MOFs (pH 7.0).

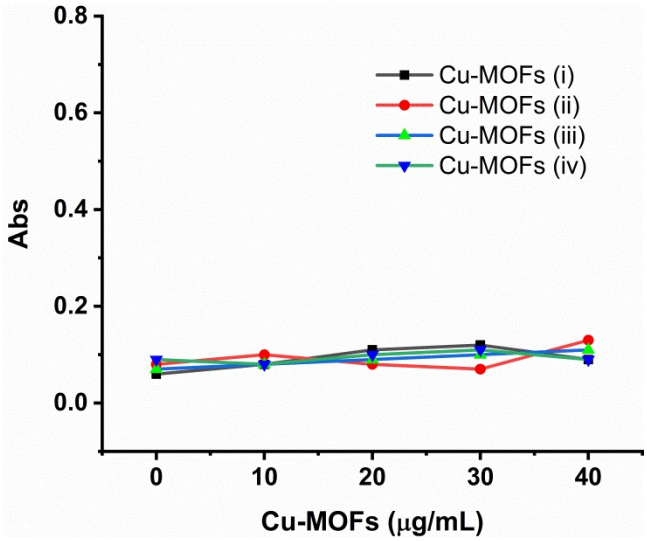

Figure S9. Study of oxidase-like properties of Cu-MOFs. Assay conditions: 0.5 mM TMB and different concentrations of Cu-MOFs (pH 7.0).

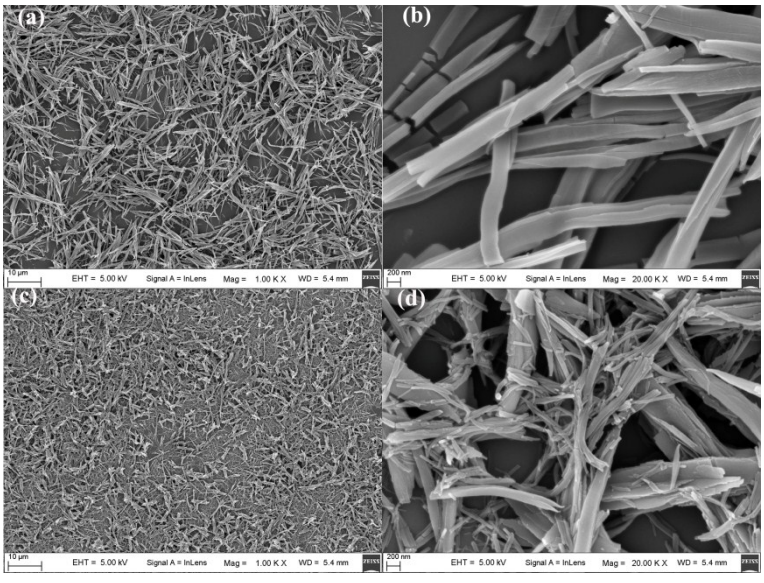

Figure S10. SEM images of Cu-MOFs (ii) before (a), (b) and after (c), (d) the catalytic reaction.

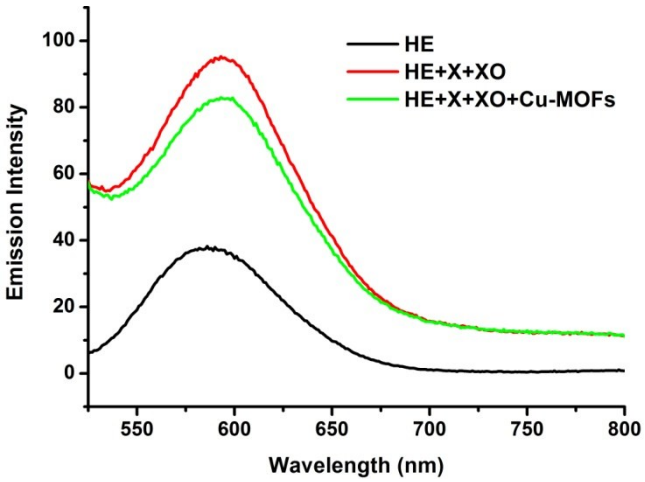

Figure S11. Effects of Cu-MOFs (ii) on the changes of $^{\bullet}O_2^-$ using dihydroethidium as the fluorescence probe. Assay conditions: 50 μM dihydroethidium, 1 mM X, 1 U/mL XO, 0.1 mM DTPA, 30 μg/mL Cu-MOFs (ii), excitation wavelength, 480 nm.

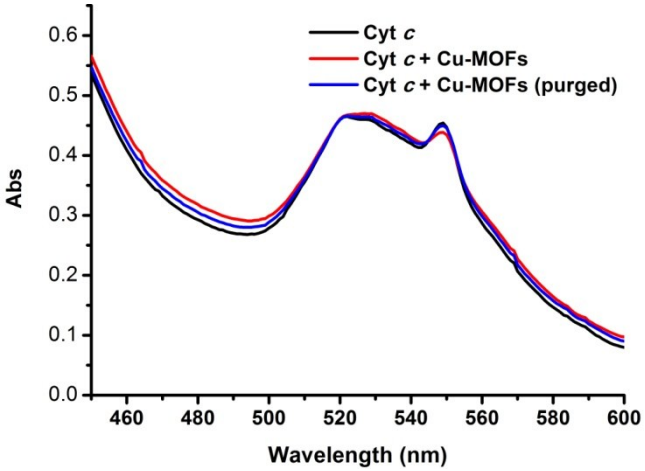

Figure S12. UV−vis spectrum of Cyt *c*, Cyt *c* reacted with Cu-MOFs (ii) and Cyt *c* reacted with Cu-MOFs (ii) under deoxygenated condition. Assay conditions: 0.5 mg/ mL Cyt *c*, 20 μg/mL Cu-MOFs (ii).

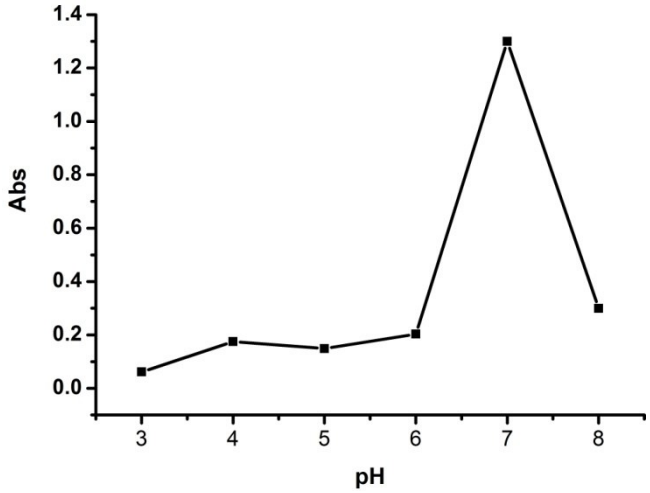

Figure S13. Effect of pH on catalytic activity of the Cu-MOFs (ii). Assay conditions: 0.5 mM TMB, 4 mM H_2O_2, 20 μg/mL Cu-MOFs (ii), 5 min.

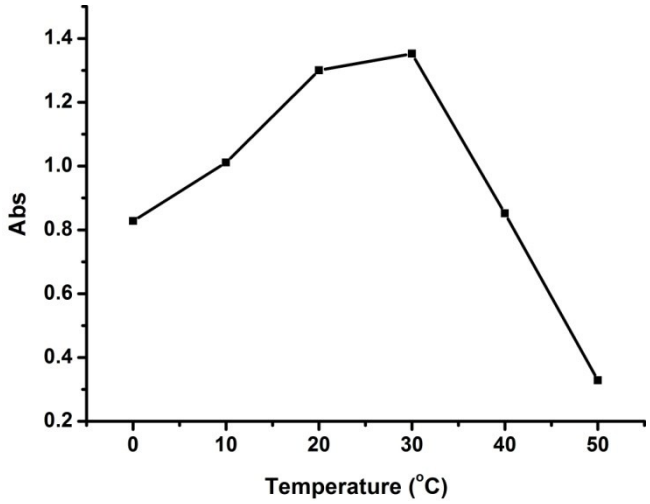

Figure S14. Dependence of the catalytic activity of Cu-MOFs (ii) on temperature. Assay conditions: 0.5 mM TMB, 4 mM H_2O_2, pH 7.0, 5 min.

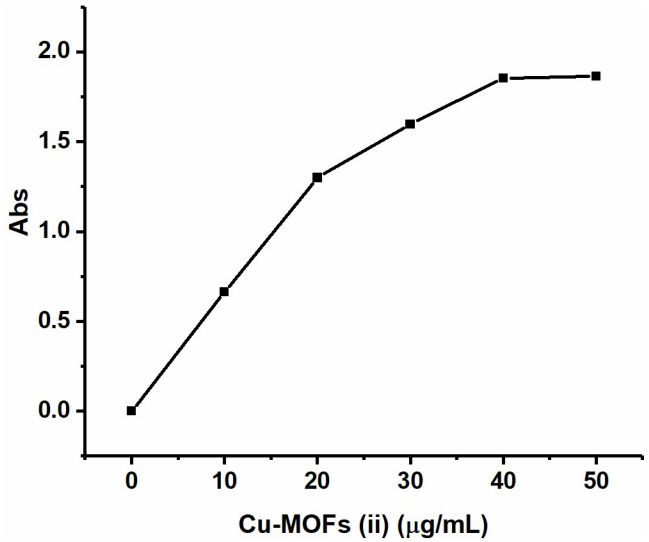

Figure S15. Effect of the amount of Cu-MOFs (ii). Assay conditions: 0.5 mM TMB, 4 mM H_2O_2, pH 7.0, 5 min.

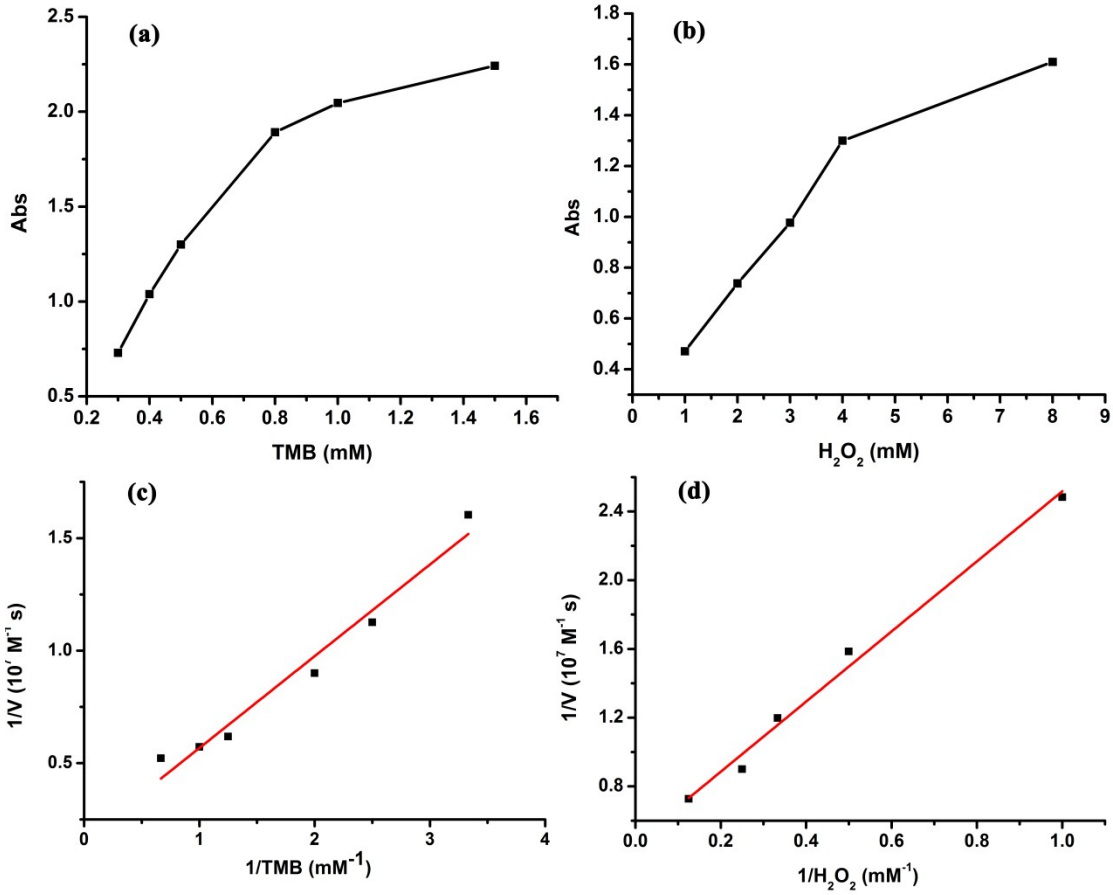

Figure S16. Steady-state kinetics measurements of the Cu-MOFs (ii). (a) The concentration of H_2O_2 was 5 mM and the TMB concentration varied. (b) The concentration of TMB was 0.5 mM and the H_2O_2 concentration varied. (c) Double reciprocal plots of activity of Cu-MOFs (ii) with the concentration of TMB varied. The TMB concentration was 0.3, 0.4, 0.5, 0.8, 1.0 and 1.5 mM, respectively. (d) Double reciprocal plots of activity of Cu-MOFs (ii) with the concentration of H_2O_2 varied. The H_2O_2 concentration was 1, 2, 3, 4 and 8 mM, respectively.

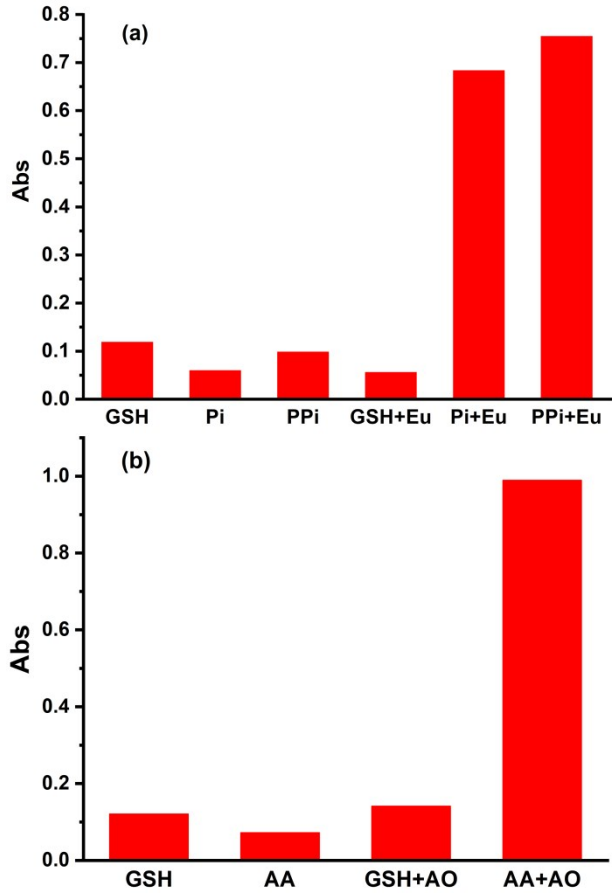

Figure S17. The effects of (a) Phosphate species or (b) ascorbic acid on GSH detection. Assay conditions: 0.5 mM TMB, 4 mM H_2O_2, 20 μg/mL Cu-MOFs (ii), 20 μM Eu^{3+}, 1 U/mL AO, 5 min.

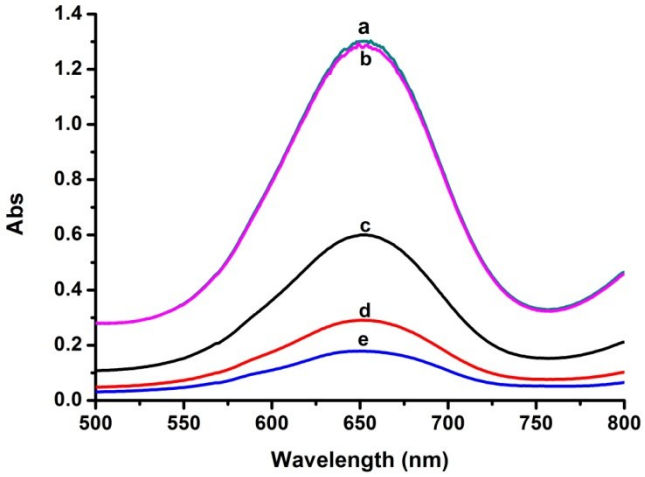

Figure S18 GSH detection in serum. line a: TMB+H_2O_2+ Cu-MOFs (ii); line b: TMB+H_2O_2+ Cu-MOFs (ii)+serum; line b: TMB+H_2O_2+ Cu-MOFs (ii)+serum+25 μM GSH; line c: TMB+H_2O_2+ Cu-MOFs (ii)+serum+55 μM GSH; line d: TMB+H_2O_2+ Cu-MOFs (ii)+serum; line e: TMB+H_2O_2+ Cu-MOFs(ii)+serum+75 μM GSH.

Table S1. Comparison of the BET surface areas and pore volumes of different Cu-MOFs.

	(i)	(ii)	(iii)	(iv)
BET Surface Area (m^2/g)	5.09	1.81	14.07	8.56

Table S2. Zeta potential of the obtained Cu-MOFs.

	1	2	3	average
Cu-MOFs (i)	-1.96	-2.04	-1.9	-1.96
Cu-MOFs (ii)	-2.6	-1.71	-2.1	-2.13
Cu-MOFs (iii)	5.56	4.96	4.6	5.04
Cu-MOFs (iv)	-20.6	4.96	-19.7	-11.78

Table S3. Comparison of the Michaelis-Menten constant (K_m) and maximum reaction rate (V_m).

catalyst	K_m (mM)		ref
	TMB	H_2O_2	
Catalase	-	4.1	37
Cu-MOFs (ii)	2.56	4.34	This work

Table S4. Absorbance of six blank samples and calculated Y axes signals

i	1	2	3	4	5	6
A_i	1.2997	1.2883	1.3021	1.2781	1.3103	1.3142
y_i=log(Ao/A)	-0.000308	0.00352	-0.00111	0.00697	-0.00384	-0.00513

Note: i represented the number of six blank samples, and A_0 was the average of six absorbance values (652 nm). And the limit of detection of calculated as follows:

$$\sigma=\sqrt{\frac{1}{n-1}\sum_{1}^{6}(y_i-y_{aver})^2}=0.0454$$

$$\mathrm{LOD}=3\times 0.00454/0.014=0.97\ (\mu\mathrm{M})$$